

# L, a, I, f i a, A, E, a, E, a M, Ma, S a

FELIX VAUX<sup>1,2,3,\*</sup>, MICHAEL R. GEMMELL<sup>1</sup>, SIMON F.K. HILLS<sup>1</sup>, BRUCE A. MARSHALL<sup>4</sup>, ALAN G. BEU<sup>5</sup>,  
JAMES S. CRAMPTON<sup>6</sup>, STEVEN A. TREWICK<sup>1</sup>, AND MARY MORGAN-RICHARDS<sup>1</sup>

<sup>1</sup> E G A E B 11-222, 4410, w ;  
<sup>2</sup>D F C E H, fi, C , 2030 E  
D, w, 97365, A; <sup>3</sup>D, 340 G K D 9016, w ;  
<sup>4</sup> w, w, w; <sup>5</sup>G B 30-368, L w H 5011, w ; <sup>6</sup> ,  
G E & E B 600, 6012, w ;  
\* C : D, 340 G K D 9016, w ;  
E- @  
01 2019; w 13 F 2020; 09 , 2020  
A E : K H,

A . .—In order to study evolutionary pattern and process, we need to be able to accurately identify species and the

is no clear temporal or spatial disjunction, or substantial morphological differences between fossil taxa, a genetic context for morphological variation is advantageous. Studies can gather this context by integrating genetic data from living relatives and the morphological analysis of both extant and fossil specimens (e.g., Stanley and Yang 1987; Jackson and Cheetham 1994; Hills et al. 2012; Smith and Hendricks 2013; Hopkins et al. 2018).

Siphon whelks from New Zealand provide an opportunity to identify evolutionary lineages using genetic and morphological data, and this knowledge can be applied to fossil material. Siphon whelks of the genus

*P. Fischer, 1884* are large marine snails (Fig. 1a) with a rich fossil record in New Zealand, including 19 extinct species, found in high abundance from many paleontological sites spanning the last 66 myr (Beu and Maxwell 1990). Although many fossils are well-preserved (Fig. 1c), evolutionary relationships among extant and fossil taxa are unclear and the taxonomic identity of specimens at many fossil sites is uncertain (Beu and Maxwell 1990). Shells exhibit considerable morphological variation in shape, size, and sculpture within and among the six extant species (and one subspecies) currently recognized in New Zealand waters (Powell 1979; Supplementary Fig. S1 available on Dryad at <http://dx.doi.org/10.5061/dryad.gqnk98sh6>), but phylogenetic analysis of mitochondrial and nuclear





TABLE 2. Sampling of extant and fossil shells

Species	Total sampling	Extant NZ	Extant species comparisons		Fossil site analyses		Lineages	
			vs. <i>fi</i>	vs. <i>te</i>	Wanganui	Te Piki	With <i>te</i>	Without <i>te</i>
<i>te</i>	125	125 (50)	125					
<i>fi</i>	238	221 (71)				200 17 <sup>†</sup>		
<i>te</i> <sup>†</sup>	7						7 <sup>†</sup>	7 <sup>†</sup>
<i>fi</i> <sup>†</sup>	4						4 <sup>†</sup>	4 <sup>†</sup>
<i>te</i>	85 (50)	78 (50)		78 7	69 7 <sup>†</sup>			
<i>fi</i>	48	48	48					
<i>te</i>	25	25						
<i>te</i> <sup>†</sup>	64						64548	54833.7(.).9748569(

of 100,000 generations and a 10% burn-in. Up to nine potential genotypic clusters were tested for ( $K = 1-9$ ). The optimal number of clusters was determined by examining estimates of posterior probability for a given value of  $K$  (Pritchard et al. 2000), and  $\Delta K$ , the rate of change in logarithmic probability of the data (Evanno et al. 2005) implemented in Structure Harvester 0.6.8 (Earl and vonHoldt 2012). Clustering for the optimal  $K$  value across the 10 replications was averaged using Clumpp 1.1.2 (Jakobsson and Rosenberg 2007), and assignment probability structure graphs were generated in DISTRUCT 1.1 (Rosenberg 2004).

## G. Geometric morphometrics

Extant and fossil shells were photographed and digitized using the same two-dimensional landmark-based geometric morphometric described in previous studies of *Hydrobia ulvae* (Vaux et al. 2017a; Vaux et al. 2018). Shells were photographed with the aperture facing upward and a total of 45 landmarks were digitized (Vaux et al. 2017a) using tpsUtil, tpsDig (Rohlf 2013) and CoordGen8 (Sheets 2014). Six landmarks and 39 semi-landmarks were used to capture the shell shape (Vaux et al. 2017a). Using this approach, experimental error during photography and digitization, respectively represented just 1.2% and 0.08% of shape variation among samples (Vaux et al. 2017a).

PCA implemented in MorphoJ 1.06c (Klingenberg 2011) was used to analyze shell shape. The PCs generated by PCA reflect mathematically independent variation in the shape of objects and centroid size acts as a proxy for size variation independent of shape (hereafter “size”). The number of PCs retained for analysis was determined using the broken-stick test on Eigenvalues for each PC. The similarity of taxa and sampling regions for shell shape was determined using ordination of the retained PCs using 90% mean confidence ellipses. In some cases, PCs were scaled with shell size using the base “scale” function in R (Becker et al. 1988; see Vaux et al. 2018), and three-dimensional scatterplots were produced using the R package car 3.0-2 (Fox and Weisberg 2011) to visualize shell shape and size variation together, with 50% confidence ellipsoids. The capacity for shell shape to distinguish groups was determined using cross-validation scores estimated by canonical variates analysis (CVA) implemented using the R package MASS 7.3-26 (Venables and Ripley 2002; R Core Team 2018) and based on PCs that in sum accounted for 95% of variation among specimens (see methods Vaux et al. 2018). CVA ordination plots were produced in MorphoJ.

To infer structure in our data sets without *a priori* identification, we employed Gaussian mixture modeling using the R package mclust 5.2 (Fraley and Raftery 2002). This approach treats the morphometric data

and *fi* (Fig. 2b). A suboptimal model for the small data set with five clusters separated all taxa, except for *fi* that was grouped with *fi* (Fig. 2c). The optimal five clusters identified for the large data set were messier with reduced assignment confidences, but supported the similar relationships and did not differentiate *fi* from *fi* or *fi* from *fi* (Fig. 2d).

The three retained PCs of shell variation mostly reflected variation in the relative height of the teleoconch spire and width of the siphonal canal and the lower part of the aperture (Supplementary Fig. S4b available on Dryad). The seven extant New Zealand taxa could not be easily distinguished using shape for 889 shells based on PCA (A791(oTJ001rg12.185817D(3(2)Tj0g0.50T;(2)Tj001626a0T;aJ001rg636ased)-247.1(on)-247.1(2)Tj1627e32g,

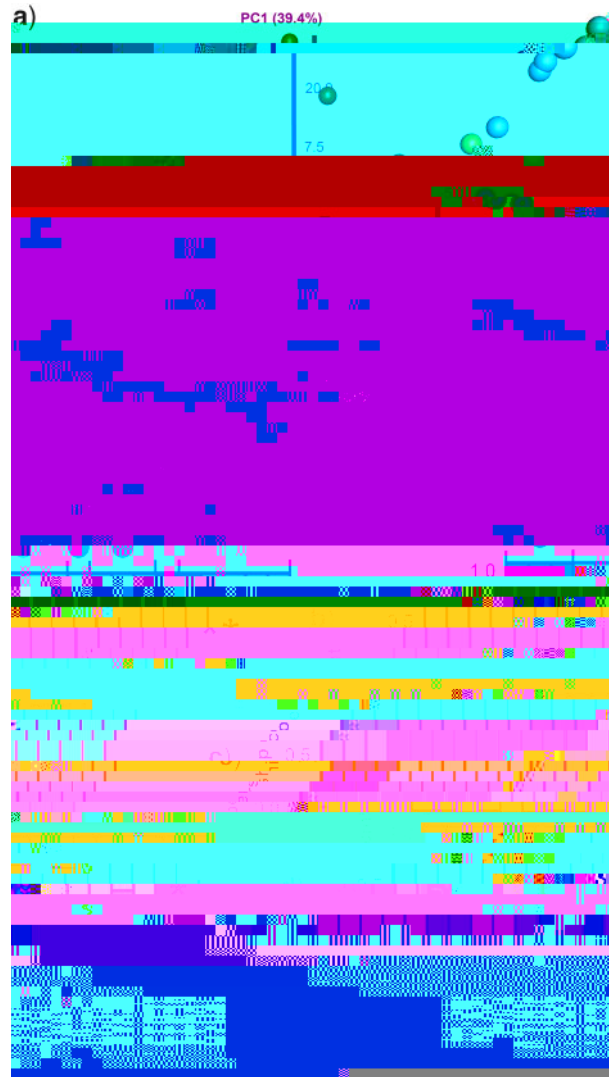


FIGURE 2. Genetic structure among a subset of New Zealand *Hydrobia ulvae* species. a) Three principal components (60% of nuclear genetic variation) separate most taxa using the large ddRAD sequencing data set of 1885 SNPs. A green arrow identifies the *H. ulvae* individual that overlaps with *H. ulvae* samples. The six currently recognized *H. ulvae* taxa are colored separately. b–d) Structure plots showing the assignment probabilities of the 18 ddRAD sequenced *H. ulvae* individuals from six taxa among estimated genotypic clusters. b and c) The optimal clustering model ( $K = 3$ ) and an alternative model ( $K = 5$ ), respectively for the small data set of 36 SNPs. d) The optimal model ( $K = 5$ ) for the large data set of 1885 SNPs.

and interpreted the likelihood of whether these four taxa belong to the same evolutionary lineage.

*Hydrobia ulvae*. We investigated morphological variation among 190 shells from Wanganui, comparing 37 fossil specimens with extant shells from 51 *H. ulvae*, 33 *H. ulvae*, and 69 *H. ulvae* snails (Table 2).



---

TABLE

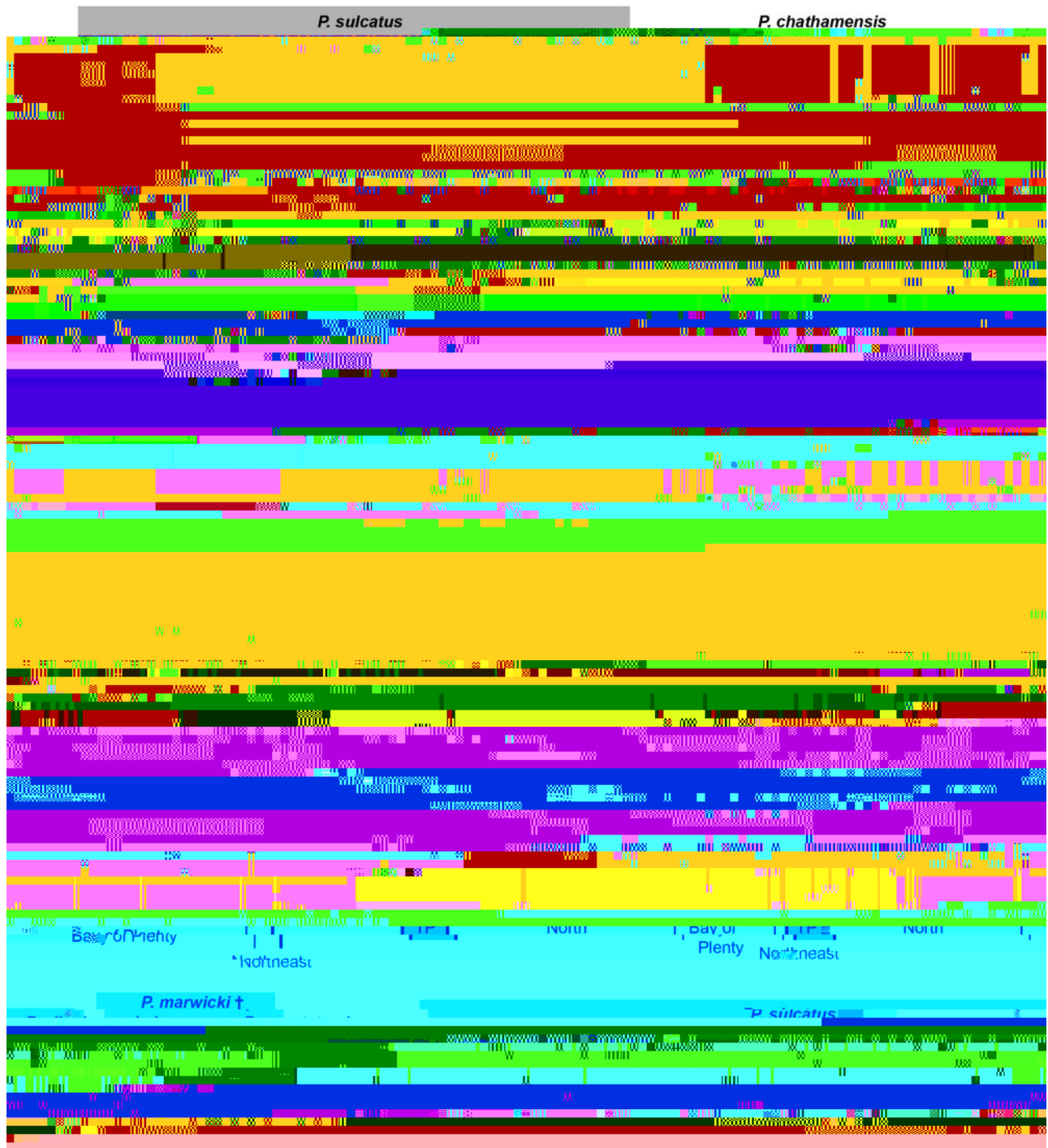


FIGURE 4. Clustering subsets of New Zealand species using Gaussian mixture modeling with shell shape and size. The optimal cluster model for each data set was estimated naïvely using the R package *mclust*. The preliminary classification of specimens and where they were collected is shown above and below each plot. (a) Comparing *P. sulcatus* and *P. chathamensis* revealed clear phenotypic distinction of these two taxa (optimal VEV2 model, using PCs 1–3 of shape, and shell size; Vaux et al. 2017a). (b) Shells of *P. sulcatus* and *P. chathamensis* were analyzed without (above) and with (below) shell size (optimal VEI2 using PCs 1–4; EEI2 using PCs 1–4 and size). (c) Analysis of *P. sulcatus* and *P. chathamensis* had poor discrimination of two taxa (optimal VVI2 model using PCs 1–4 and size). (d) An analysis combining fossils from Wanganui with modern shells of *P. sulcatus*, *P. chathamensis*, and *P. marwicki* from adjacent regions (optimal VEE3 model using PCs 1–4 and size). (e) An analysis combining fossils from Te Piki with modern shells of *P. sulcatus* and *P. chathamensis* from adjacent regions (EEI2 using PCs 1–3). (f) An analysis combining reclassified shells of extant and fossil *P. sulcatus*, and fossils of the extinct species *P. marwicki*, *P. chathamensis*, and *P. sulcatus* (EEE2 using PCs 1–3). Alternative Gaussian mixture (*mclust*) models and Bayesian information criteria support for each data set are provided in the [Supplementary Material](#) available on Dryad.



on Dryad). PC2 for each data set represented almost identical amounts of shell shape variation (21.8% with  $\dots$ , 21.7% without  $\dots$ ; Table 3), and both reflected variation in the relative height of the teleoconch spire and aperture (with  $\dots$  included shown in [Supplementary Fig. S19d](#) available on Dryad). We therefore consider PC2 in each data set to be comparable. Overall, the choice of whether to include  $\dots$  6.1(r)4.38hn1.05TDgdMdTDyse002Tc0002olutionary11.05TDgdMdTDkse002ey detrminantherfphological stasis was detected.

## DISCUSSION

Integrating data from living and extinct species will help to detrmine the ext to which species diversification and phenotypic eTc0092olution are coupled in the natural wTc0072ogd0.3(r)20072ld, which igd0.3(s)-211.4(r)4.7TDq before the drivers ogd0.3(f)-211.4(e)11.7(vTc0072olution-)]TJT\*0Tc[ betwgandmorphometricvariationinextant populations, followd bycomparisonofmorphological variation betw modern and fossil populations, in order to resolvuncertahn species identification in fossil deposits.evhatorhhe genus provides a useful case study for the integration of extant andxtincterialoresearchvy

In f.50s(11.05TDgd394.8(more)-394.8(s)14.8(tr)-9.2(ing)18.8TDnt)-394.8(ddRAD)-394.7(data)-394.8(s).05TDt, using fyse002 anonymous nuclear SNPs, most of the currDntly recognized extant species of N Zealand 6er

orw

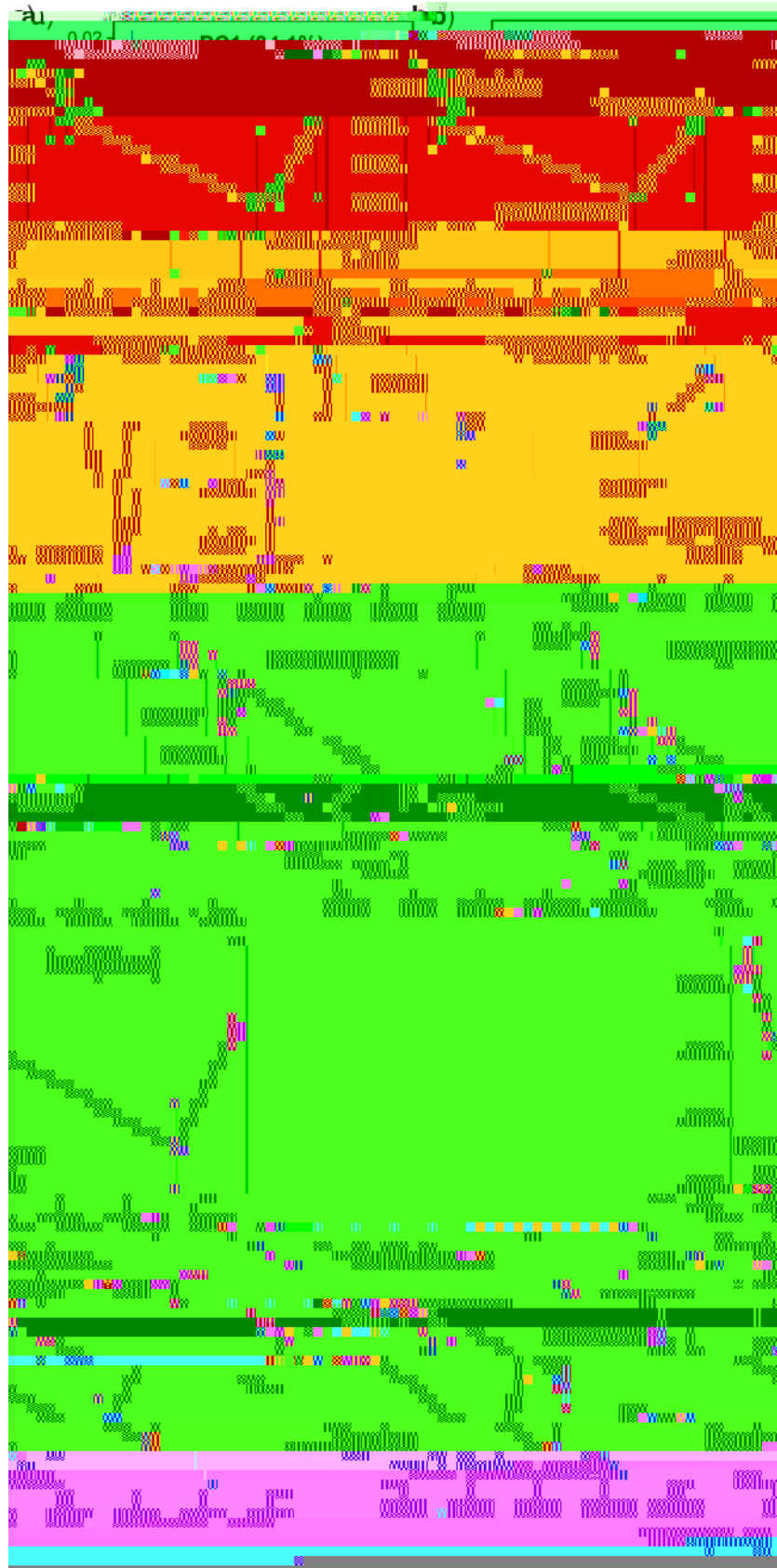


FIGURE 6. Time series analyses of shell shape and size evolution estimated for two alternative lineages over 20 myr (results from paleoTS). The best fitting model of evolutionary mode is labeled for each analyzed trait (retained shell shape PCs and shell size). a) Evolutionary lineage consisting of *Tridacna*, *Tridacna*, and *Tridacna*; each shown in a different color. b) Evolutionary lineage consisting of *Tridacna*, *Tridacna*, and *Tridacna*. Full paleoTS results including support values for each evolutionary model per trait are provided in [Supplementary Tables S8 and S9](#) available on Dryad.

suggest that these fossils represent a single lineage, compatible with molecular clock analysis that estimated the age for the most recent common ancestor of *Stylidium* and other New Zealand *Stylidium* species long before the oldest fossil *Stylidium* or *Stylidium* (median 40.6 Ma; 95% HPD 49.8–32.1 Ma; [Vaux et al. 2017b](#)). Considering that shell morphology and evolutionary relationships appear to be concordant in *Stylidium*, this result is remarkable as it suggests that no substantial morphological change has occurred in the Biology

## REFERENCES

- Abdelkrim J., Aznar-Cormano L., Buge B., Fedosov A., Kantor Y., Zaharias P., Puillandre N. 2018. Delimiting species of marine gastropods (Turridae, Conoidea) using RAD sequencing in an integrative taxonomy framework. *Mol. Ecol.* 27:4591–4611.
- Agapow P-M., Bininda-Emonds O.R.P., Crandal K.A., Gittleman J.L., Mace G.M., Marshall J.C., Purvis A. 2004. The impact of species concept on biodiversity studies. *Q. Rev. Biol.* 79:161–179.

